Coexistence and $2' \rightarrow 2_1$ $E2$ strengths

H. T. Fortune
Department of Physics and Astronomy, University of Pennsylvania, Philadelphia, Pennsylvania 19104, USA

(Received 4 September 2019; published 5 November 2019)

I have used parameters previously determined from a simple mixing analysis of $0 \leftrightarrow 2$ transition strengths in several nuclei to compute $E2$ transition matrix elements for the 2_2 (or 2_3, as determined by the experimenters) $\rightarrow$ 2_1 transition. Agreement with experimental $E2$ transition matrix elements is reasonable.

DOI: 10.1103/PhysRevC.100.054305

I. INTRODUCTION

Many nuclei exhibit two sets of states at low excitation, with each group containing $J^\pi = 0^+, 2^+, 4^+, \ldots$. This phenomenon is sometimes called shape coexistence, or phase coexistence, or just coexistence. Heyde and Wood and co-workers have written extensively on the subject [1]. Frequently, these two sets of states have quite different structure, usually with some amount of mixing between them. Many of these cases have been successfully described in terms of a simple two-state mixing model, which allows each pair of states to mix. The model is characterized by strong $E2$ transitions within each group, but negligible transitions between the groups.

For example, four $E2$ transition matrix elements describe the $0 \leftrightarrow 2$ transitions, and the 0^+ and 2^+ mixing contains four parameters to be determined: two mixing amplitudes and two basis-state $E2$ matrix elements. I write

$$0_1 = a\,0_g + b\,0_e, \quad 0_2 = -b\,0_g + a\,0_e,$$
$$2_1 = A\,2_g + B\,2_e, \quad 2_2 = -B\,2_g + A\,2_e;$$

and I define $M_g = \langle 0_g \| E2 \| 2_g \rangle$, $M_e = \langle 0_e \| E2 \| 2_e \rangle$. Then, one finds

$M(E2; 2_1 \rightarrow 0_1) = aAM_g + bBM_e$, and similarly for the other transitions.

II. DATA AND ANALYSIS

I have used this model to analyze several nuclei. Frequently, the experimenters indicated that it is the third 2^+ state (rather than the second one) that is to be associated with the second 0^+ state. I followed their recommendations in all cases. I have used the notation $2'$ to denote either 2_2 or 2_3; whichever the experimenters determined as associated with the excited 0^+ state. The tables indicate the choice for each nucleus.

In my earlier analysis, I ignored the 2_i to 2_f transitions, which I address here. For a $K = 0$ rotational band, one finds $\langle 2 \| E2 \| 2 \rangle = (10/7)^{1/2} \langle 0 \| E2 \| 2 \rangle$ [2]. This is equivalent to the perhaps more familiar expressions [3]

$$\langle 0 \| E2 \| 2 \rangle = (5/16\pi)^{1/2} Q_0$$

and

$$Q(2^+) = -(2/7)Q_0 = 0.758 \langle 2 \| E2 \| 2 \rangle = -0.906 \langle 0 \| E2 \| 2 \rangle,$$

where Q_0 is the intrinsic quadrupole moment of the 2^+ state and $Q(2^+)$ is the electric quadrupole moment of the 2^+ state. Thus, with the 2^+ wave functions above,

$$|M(E2;\, 2_2 \rightarrow\, 2_1)| = (10/7)^{1/2} AB |M_g - M_e|.$$

For several nuclei from ^{42}Ca to ^{154}Gd, I have evaluated this expression, using published values [4–10] for A, B, M_g, and M_e (Tables I and II), and compared results with known experimental matrix elements [11–19]. Results are listed in Tables III and IV and plotted in Figs. 1 and 2. Overall agreement is satisfactory. Agreement is good for ^{74,76}Kr, but significantly worse for ^{78}Kr. Agreement is very good for ^{152}Sm and ^{154}Gd, but worse for ^{106,108}Pd. The fact that the calculated values are larger than the experimental ones in Pd might indicate the presence of another (vibrational?) amplitude that interferes destructively. Also, the properties of the e band that emerged from the fit in ^{106}Pd did not have the properties of a $K = 0$ rotational band. Of course, ^{106,108}Pd are closer to vibrational than any of the other nuclei considered here.

TABLE I. For selected nuclei with $A < 100$, 2^+ mixing amplitudes and $0 \leftrightarrow 2$ basis-state $E2$ transition matrix elements from previous mixing analyses.

Nucl.	i	A	B	M_g (eb)	M_e (eb)	Ref.
^{42}Ca	2_2	0.657	0.754	0.0999	0.391	[4]
^{72}Ge	2_3	0.930	0.367	0.615	0.182	[5]
^{74}Kr	2_2	0.906(9)	0.423	1.14	0.211	[6]
^{76}Kr	2_3	0.800(10)	0.600	1.097	0.727	[6]
^{78}Kr	2_3	0.956(24)	0.293	0.912	0.175	[6]
^{98}Sr	2_2	0.998	0.054	1.245	0.374	[7]

TABLE II. For selected nuclei with $A > 100$, 2^+ mixing amplitudes and $0 \leftrightarrow 2$ basis-state $E2$ transition matrix elements from previous mixing analyses.

Nucl.	i	A	B	M_g [(W.u.)$^{1/2}$]	M_e [(W.u.)$^{1/2}$]	Ref.
^{106}Pd	2_3	0.815	0.579	17.98	11.12	[8]
^{108}Pd	2_3	0.715	0.699	20.82	12.81	[8]
^{152}Sm	2_2	0.851	0.525	29.5	21.0	[9]
^{154}Gd	2_2	0.808	0.589	31.9	22.4	[10]

TABLE III. For selected nuclei with $A < 100$, $E2$ transition matrix elements for the 2_2 (or 2_3) $\rightarrow 2_1$ transition.

			$\lvert M(E2)\rvert$ (eb)			
Nucl.	i	f	Exp.	Calc.[a]	Other	Model
^{42}Ca [11]	2_2	2_1	$0.237^{+0.023}_{-0.027}$	0.172	0.136	SM[b]
					0.077	BMF[c]
^{72}Ge [12]	2_3	2_1	$0.243^{+0.002}_{-0.004}$	0.177	0.08	TRM[d]
^{74}Kr [13]	2_2	2_1	0.49(4)	0.43	0.53	Skyrme [13]
					0.94	Gogny [13]
^{76}Kr [13]	2_3	2_1	$0.200^{+0.004}_{-0.008}$	0.212	0.64	Skyrme [13]
					0.017	Gogny [13]
^{78}Kr [14]	2_3	2_1	$0.50^{+0.02}_{-0.05}$	0.25	0.12	EXVAM[e]
^{98}Sr [15]	2_2	2_1	$0.07^{+0.10}_{-0.05}$	0.063	0.10	5DCH[f]

[a]Present.
[b]Shell model [11].
[c]Beyond mean field [11].
[d]Triaxial rotor model [12].
[e]Excited VAMPIR (mixing configurations with different deformation) [12].
[f]Five-dimensional collective Hamiltonian [13].

TABLE IV. For selected nuclei with $A > 100$, $E2$ transition matrix elements for the 2_2 (or 2_3) $\rightarrow 2_1$ transition.

			$M(E2)$ [(W.u.)$^{1/2}$]			
Nucl.	i	f	Exp.	Calc.[a]	Other	Model
^{106}Pd [17]	2_3	2_1	$1.61^{+0.20}_{-0.16}$	3.87	0	HV[b]
^{108}Pd [17]	2_3	2_1	$2.94^{+0.17}_{-0.61}$	4.72	0	HV[b]
^{152}Sm [18]	2_2	2_1	5.24(24)	4.88	7.1	IBA[c]
					5.48	PPQ[d]
					6.7	GCM[e]
					8.1	$X(5)$
^{154}Gd [19]	2_2	2_1	5.61(18)	5.40	6.9	IBA[c]
					12	GCM[e]
					8.4	$X(5)$

[a]Present.
[b]Harmonic vibrator [17].
[c]Interacting boson approximation [18,19].
[d]Pairing plus quadrupole [18].
[e]Geometric collective model [18,19].

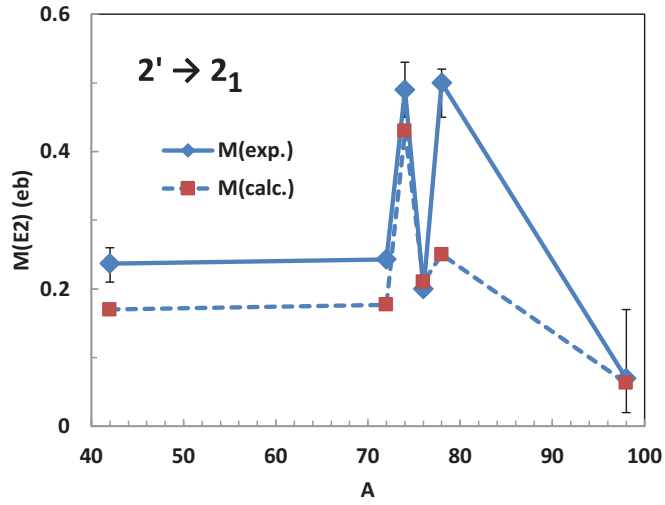

FIG. 1. Experimental (diamonds) and calculated (squares) $E2$ transition matrix elements for $2' \rightarrow 2_1$ transitions in selected nuclei with $A < 100$. Lines serve only to connect the points. The notation $2'$ denotes either 2_2 or 2_3 (see tables) as determined by the experimenters.

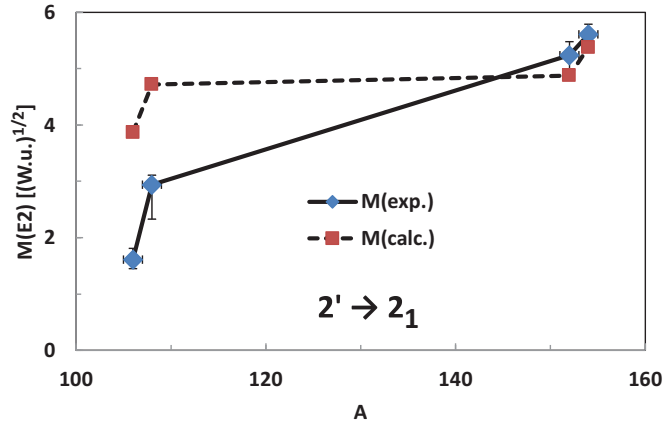

FIG. 2. As in Fig. 1, but for $A > 100$.

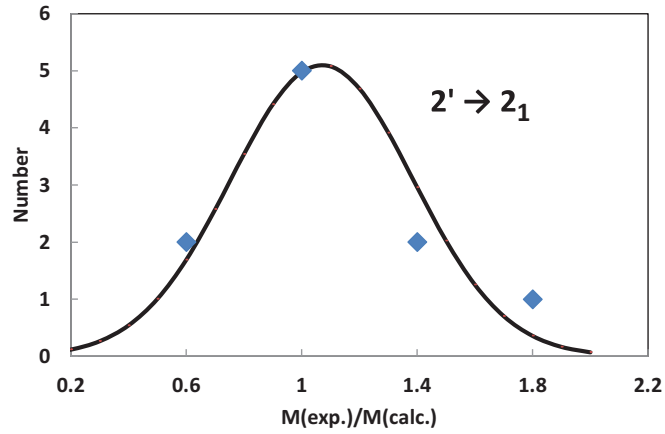

FIG. 3. Frequency distribution of M(exp.)/M(calc.), compared to normal Gaussian.

The average value of M(exp.)/M(calc.) is 1.11, with a standard deviation of 0.43. I have binned the ratios and plotted the frequency distribution in Fig. 3. It can be noted that the distribution is well fitted by a normal Gaussian shape.

The tables also contain calculated $2' \rightarrow 2_1$ $E2$ transition matrix elements from a variety of models that were considered in the experimental papers. With a few exceptions, these are generally in poorer agreement with experimental values than are the ones I have computed here. I emphasize there are no free parameters in the present calculations. All parameters are taken from earlier analyses.

III. SUMMARY

In several nuclei, I have computed $E2$ transition matrix elements for the 2_2 (or 2_3, as determined by the experimenters) $\rightarrow$ 2_1 transition, using parameters previously determined from a simple mixing analysis of $0 \leftrightarrow 2$ transition strengths in these nuclei. Agreement with experimental values is reasonable.

ACKNOWLEDGMENT

I am grateful to Larry Zamick for useful correspondence.

[1] K. Heyde and J. L. Wood, Rev. Mod. Phys. **83**, 1467 (2011), and references therein.
[2] A. de Shalit and H. Feshbach, *Theoretical Nuclear Physics* (John Wiley and Sons, New York, 1974), Vol. I, p. 411.
[3] Y. Y. Sharon, N. Benczer-Koller, G. J. Kumbartzki, L. Zamick, and R. F. Casten, Nucl. Phys. A **980**, 131 (2018).
[4] H. T. Fortune, Nucl. Phys. A **962**, 1 (2017).
[5] H. T. Fortune, Phys. Rev. C **94**, 024318 (2016).
[6] H. T. Fortune, Eur. Phys. J. A **54**, 229 (2018).
[7] H. T. Fortune, Nucl. Phys. A **957**, 184 (2017).
[8] H. T. Fortune, Phys. Rev. C **98**, 064303 (2018).
[9] H. T. Fortune, Nucl. Phys. A **966**, 47 (2017).
[10] H. T. Fortune, Eur. Phys. J. A **54**, 178 (2018).
[11] K. Hadyńska-Klęk *et al.*, Phys. Rev. Lett. **117**, 062501 (2016).
[12] A. D. Ayangeakaa *et al.*, Phys. Lett. B **754**, 254 (2016).
[13] E. Clement *et al.*, Phys. Rev. C **75**, 054313 (2007).
[14] F. Becker *et al.*, Nucl. Phys. A **770**, 107 (2006).
[15] E. Clément *et al.*, Phys. Rev. Lett. **116**, 022701 (2016).
[16] L. E. Svensson *et al.*, Nucl. Phys. A **584**, 547 (1995).
[17] F. M. Prados-Estévez *et al.*, Phys. Rev. C **95**, 034328 (2017).
[18] R. M. Clark, M. Cromaz, M. A. Deleplanque, R. M. Diamond, P. Fallon, A. Görgen, I. Y. Lee, A. O. Macchiavelli, F. S. Stephens, and D. Ward, Phys. Rev. C **67**, 041302(R) (2003).
[19] D. Tonev, A. Dewald, T. Klug, P. Petkov, J. Jolie, A. Fitzler, O. Möller, S. Heinze, P. von Brentano, and R. F. Casten, Phys. Rev. C **69**, 034334 (2004).